

STRUCTURAL RESPONSE OF BEAD-STIFFENED THERMOPLASTIC SHEAR WEBS

Marshall Rouse
NASA Langley Research Center
Hampton, VA

22-24
1/1/73

INTRODUCTION

Advanced composite materials offer an attractive potential for reducing the mass of modern aircraft structural components. To achieve this potential, the ability to provide reliable structural designs that can safely carry the desired loads must be developed. Current design practices allow some metallic structural components (e.g., fuselage and stabilizer panels) to buckle under various loading conditions and, as a result, are said to have postbuckling strength. The corresponding structural response characteristics of graphite-thermoplastic composites must be evaluated before such composites can be considered for application to civil transport aircraft structures. One aspect of the design of aircraft structural components is the structural behavior of panels loaded in shear. Experimental results have been presented that describe buckling and postbuckling behavior of graphite-epoxy and graphite-thermoplastic specimens under various loading conditions (References 1 and 2). An advanced concept for stiffened graphite-thermoplastic panels is a thermoformed bead-stiffener. The thermoforming process is a potentially cost-effective manufacturing technique for these bead stiffeners. The postbuckling response of bead-stiffened graphite-thermoplastic shear webs has not been fully described. The influences of local effects, such as bead-stiffener geometry and orientation, on the postbuckling response of graphite-thermoplastic shear webs has also not been adequately described.

The present paper describes the results of an experimental and analytical study of the structural response and failure characteristics of selected bead-stiffened thermoplastic shear webs. Experimental results are presented for specimens with one stiffener, two stiffeners, and different stiffener geometries. Selected analytical results that were obtained with the Computational Structural Mechanics (CSM) Testbed (Ref. 3) computer code are presented. Analytical results that describe normal and transverse shear stress resultants are also presented.

TEST SPECIMEN DESCRIPTION

The graphite-thermoplastic specimens tested in this investigation were fabricated from commercially available unidirectional tapes of Hercules Incorporated AS4 graphite fiber and ICI ACP PEEK resin. All of the specimens tested in this investigation were made from 16-ply laminates with a $[\pm 45_2/0/\pm 45/90]_S$ stacking sequence. The specimens had a 12-inch by 12-inch test section and the edges were reinforced with fiberglass reinforcements bonded to the specimens with a room-temperature-cure adhesive. A total of three specimens were tested in this investigation. All of the specimens were tested had bead stiffeners oriented parallel to one side of the specimen. The bead stiffeners had an 11-inch length, 0.5-inch height, and a stiffener width b_S of either 2 or 3 inches. One specimen was tested with one 3-inch-wide bead stiffener located at the center of the test section. Two specimens were tested with two bead stiffeners located 3.5 inches from the edges of the test section. One of the two-stiffener specimens had 2-inch-wide bead stiffeners and the other specimen had 3-inch-wide bead stiffeners. Photographs of specimens with one and two bead stiffeners are shown in Figure 1.

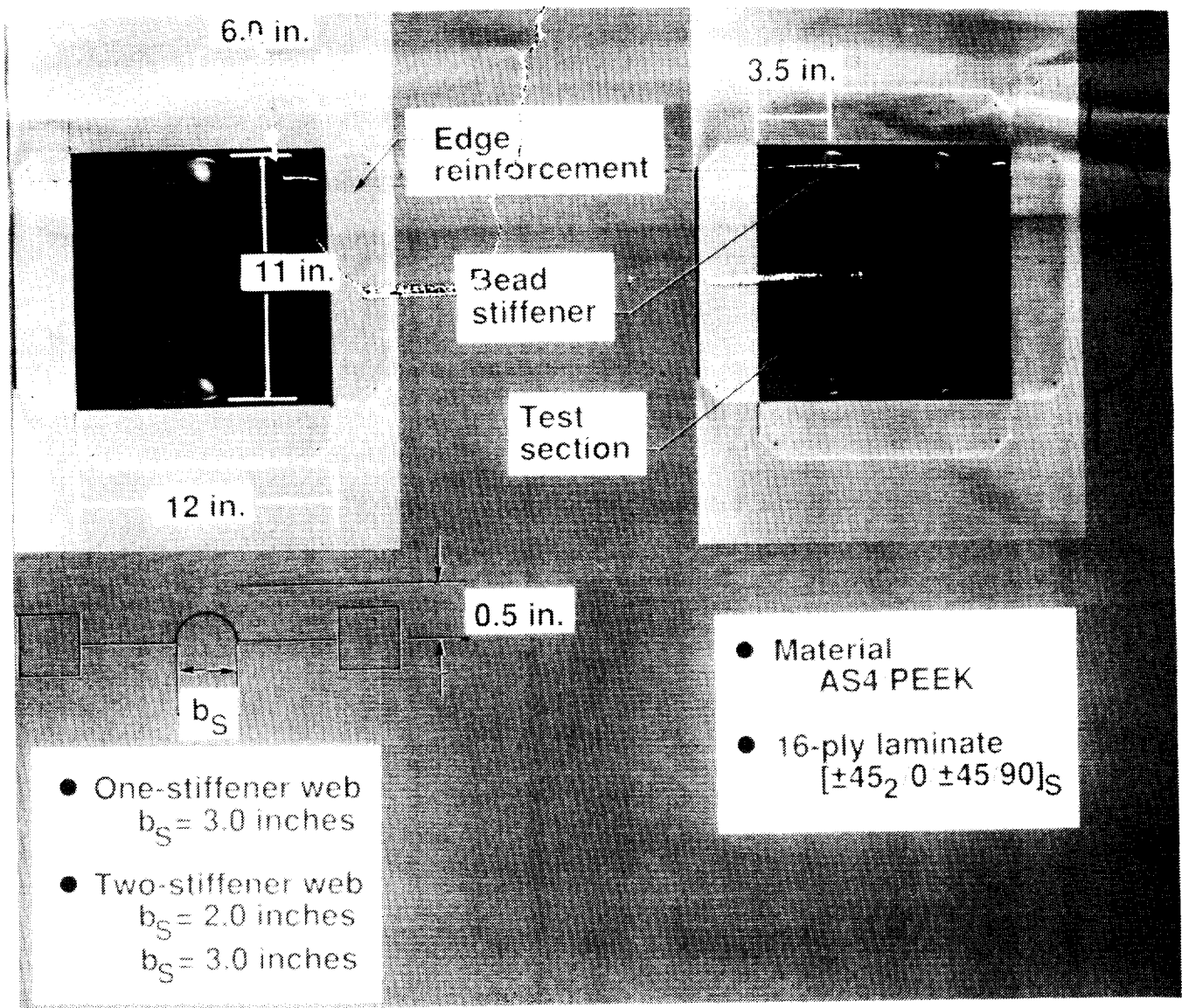


Figure 1

SUMMARY OF TEST RESULTS FOR BEAD-STIFFENED WEBS

A summary of results for all of the bead-stiffened shear webs that were tested is shown in Figure 2. All of the specimens were tested using a picture-frame fixture which is composed of two back-to-back steel rails bolted to the edge reinforcements on each specimen edge. The rails are connected with high strength pins, and the pins are positioned with their center lines coincident with the corners of the test section of the specimen. A uniaxial loading condition was used to test each specimen. The uniaxial loading condition consisted of applying a tension load P along one diagonal of the specimen. The sketch on the left of Figure 2 illustrates the applied load P . The applied shear flow q was calculated from the applied load by imposing equilibrium conditions on the test section of the specimen and by assuming that the picture-frame fixture and edge reinforcements are rigid and pinned at the corners.

Applied shear flow q as a function of extension along the diagonal δ in the direction of the applied load is shown on the right of the figure. The theoretical shear flow at buckling for the specimen with one bead stiffener (one-stiffener web) is indicated in the figure by the open circle. Only the specimen with one centrally located stiffener failed at an applied load greater than the theoretical buckling load. Failure of the specimen with one bead stiffener is indicated by the filled circle. Failure of the specimens with two bead stiffeners (two-stiffener web) is indicated by the filled squares. The specimen with one 3-inch-wide bead buckled at an applied shear flow of approximately 1,000 lb/in. and failed at an applied shear flow of approximately 1,500 lb/in. The specimens that were tested with two bead stiffeners failed prior to buckling. The two-stiffener specimens with 2-inch-wide bead stiffeners and 3-inch-wide stiffeners failed at a value of applied shear flow of approximately 1,400 lb/in. and 1,900 lb/in., respectively.

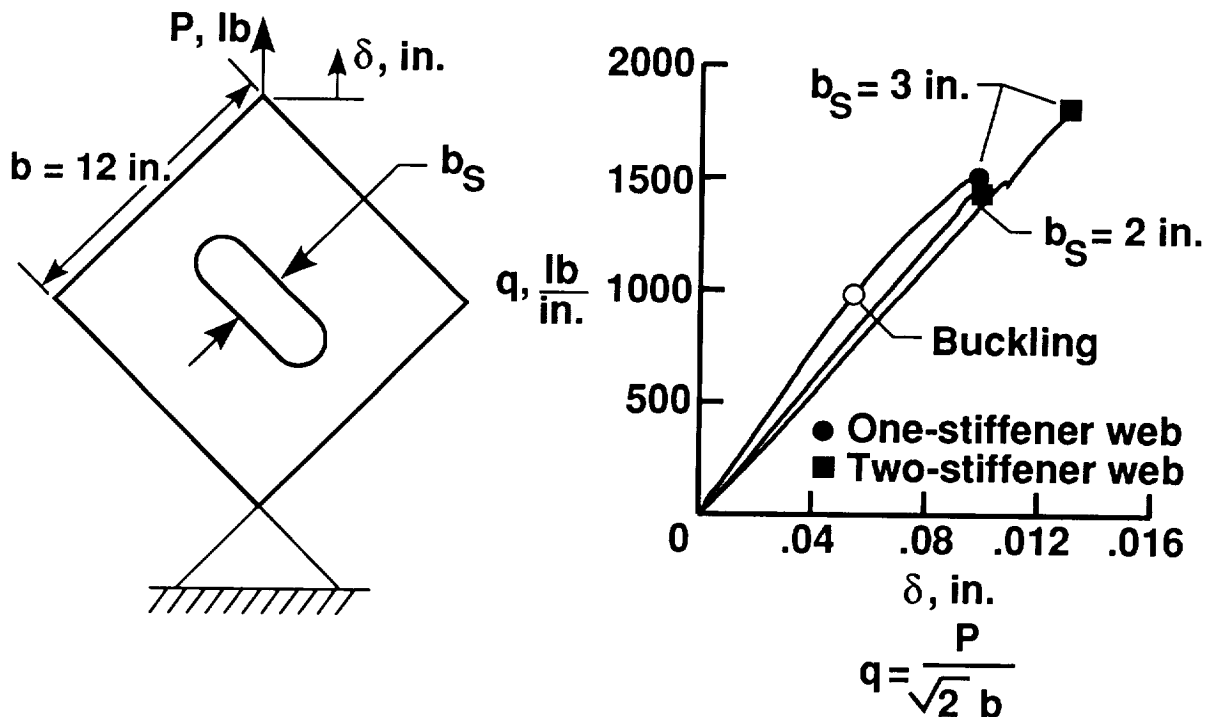


Figure 2

OUT-OF-PLANE DEFLECTION OF BEAD-STIFFENED WEBS

Out-of-plane deflection w was measured at the center of a bead normalized by the laminate thickness t is shown in Figure 3 as a function of applied shear flow q for all of the specimens that were tested. Failure of the one-stiffener specimen is indicated by the filled circle. Failure of the two-stiffener specimens is indicated by the filled squares. All of the specimens deformed out-of-plane when loaded. Photographs of typical moiré-fringe patterns for a one-stiffener and a two-stiffener specimen are shown on the right of the figure. The one-stiffener specimen with a 3-inch-wide bead stiffener exhibited the most out-of-plane deflection during loading with a maximum value of almost 10 times the laminate thickness. The two-stiffener specimens with 2- and 3-inch-wide bead stiffeners had a maximum out-of-plane deflection of approximately two and one times the laminates thickness, respectively. The change in slope of the curves shown in Figure 3 suggests that the bead-stiffened webs have a nonlinear response when loaded to failure.

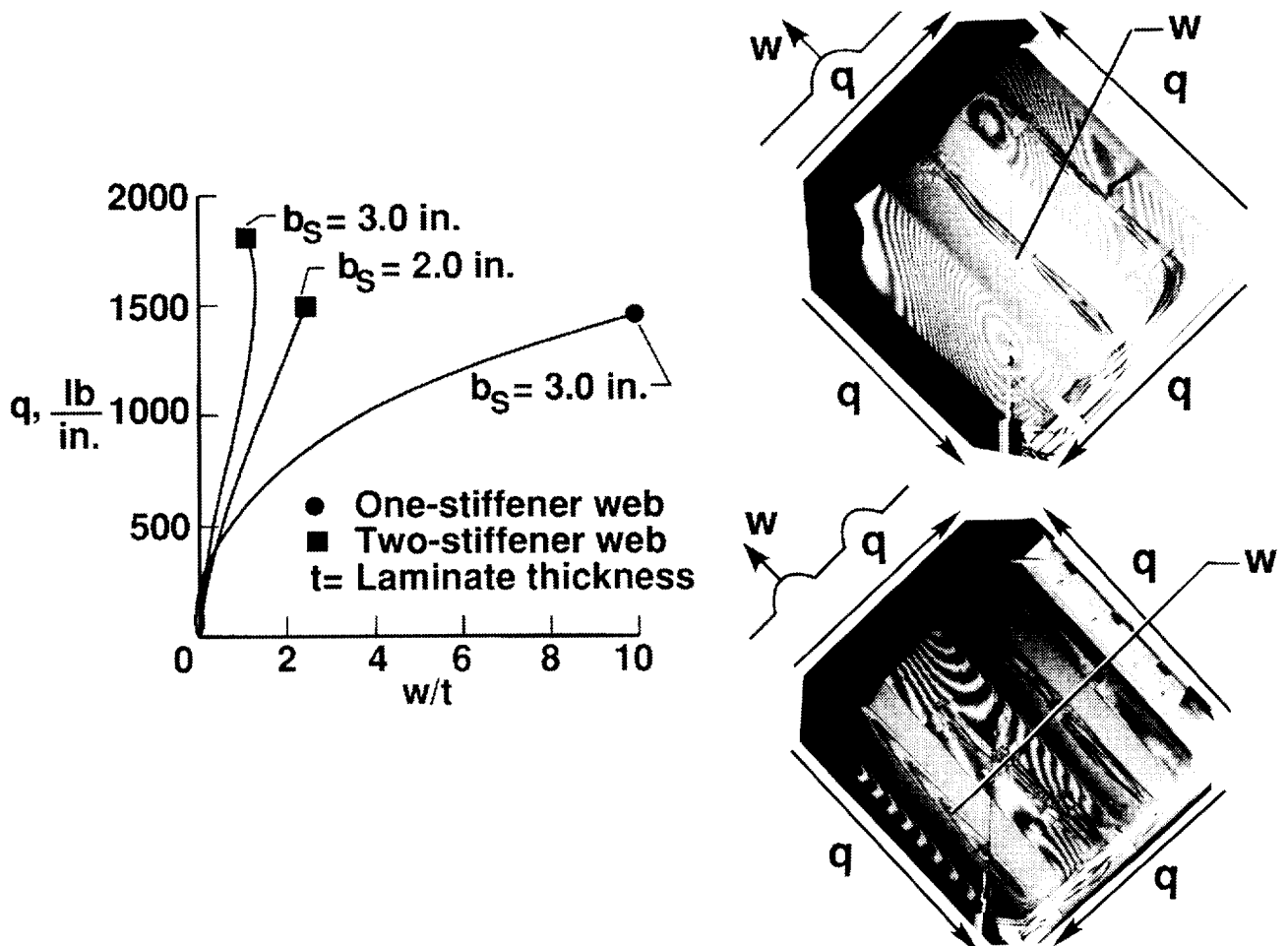


Figure 3

BACK-TO-BACK SURFACE STRAIN RESULTS FOR WEBS WITH 3-INCH-WIDE STIFFENERS

A comparison of surface strain results for one- and two-stiffener specimens with 3-inch-wide stiffeners is presented in Figure 4 as a function of applied shear flow q . The surface strains ϵ were recorded from back-to-back strain gage rosettes located at the center of a bead stiffener. Results for the one-stiffener specimen are indicated by the filled circles. Results for the two-stiffener specimens are indicated by the filled square. Surface strain measurements ϵ_t from strain gages oriented parallel to the direction of applied load are shown in the upper left of the figure. The one-stiffener specimen had a maximum tensile strain approximately of 0.006 in./in. at failure. The two-stiffener specimen had a maximum tensile strain value of approximately 0.004 in./in. at failure. Surface strain measurements ϵ_c from strain gages oriented normal to the direction of applied load are shown in the upper right of the figure. The one- and two-stiffener specimens had a maximum compressive strain of approximately -0.001 in./in. and -0.004 in./in., respectively. The change in slope of the curve for the one-stiffener specimen suggests a nonlinear load-strain response. The divergence of the back-to-back strain gage results also suggests that bending strains occur at the center of the bead stiffener in the direction of applied load and increase as the specimen is loaded to failure. Surface strain measurements ϵ_x from back-to-back strain gages oriented parallel to the longitudinal direction of the stiffener are shown in the lower left of the figure. The one-stiffener specimen had a maximum strain value in the x-direction of approximately 0.004 in./in. at failure. The two-stiffener specimen had a maximum strain value of approximately 0.001 in./in. at failure. Also, the change in slope of the curves suggests that the load in the stiffeners was redistributed as the specimen was loaded to failure.

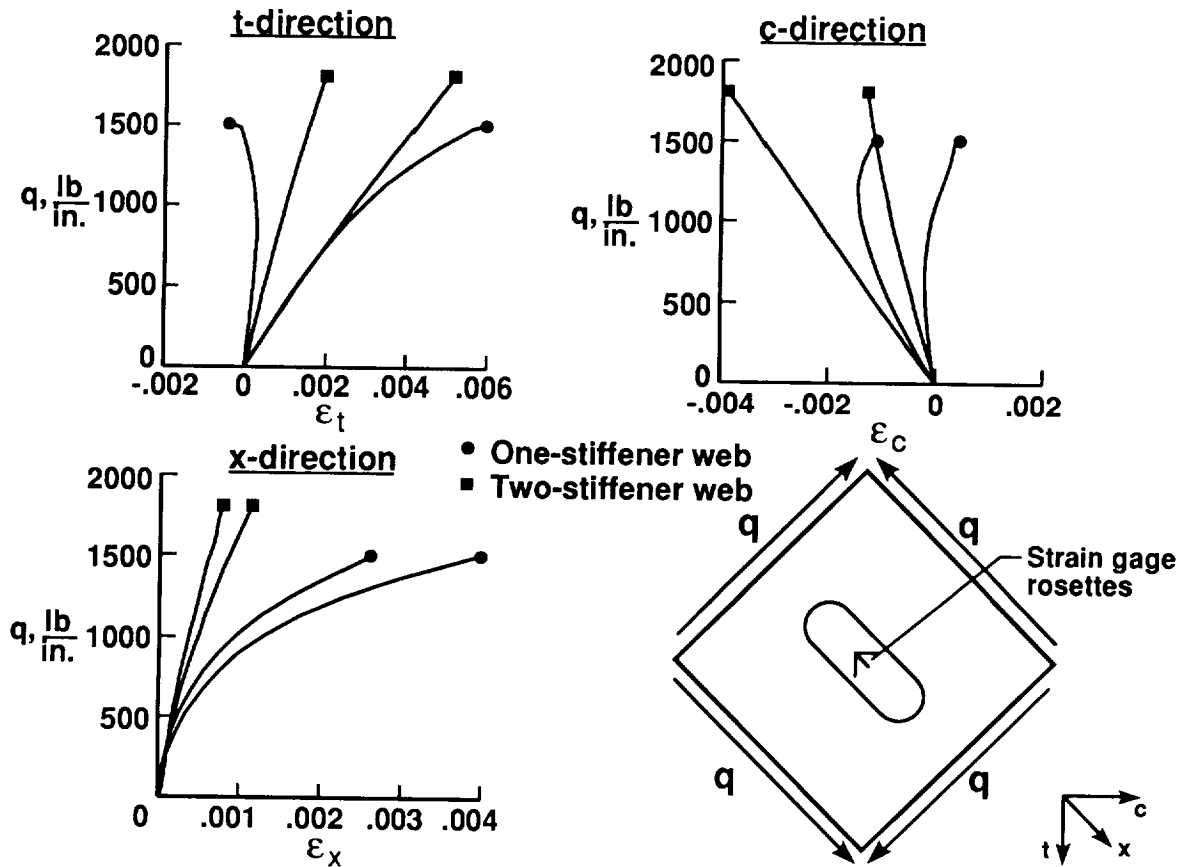


Figure 4

BACK-TO-BACK SURFACE STRAIN RESULTS FOR WEBS WITH TWO STIFFENERS

A comparison of surface strain results for two-stiffener specimens with 2- and 3-inch-wide (b_s) stiffeners are presented in Figure 5 as a function of applied shear flow q . The surface strains ϵ were recorded from back-to-back strain gage rosettes located at the center of a bead stiffener. Results for a two-stiffener specimen with 2.0-inch-wide stiffeners are indicated by the filled circle. Results for the two-stiffener specimens with 3-inch-wide stiffeners are indicated by the filled square. Surface strain measurements ϵ_t from strain gages oriented parallel to the direction of applied load are shown in the upper left of the figure. Back-to-back surface strain results in the t-direction indicate that two-stiffeners specimens with 2- and 3-inch-wide stiffeners had the same load-strain response up to failure. However, the two-stiffener specimen with 3-inch-wide stiffeners failed at higher values of applied shear flow and tension strain. Surface strain measurements ϵ_c from strain gages oriented normal to the direction of applied load are shown in the upper right of Figure 5. Back-to-back surface strain results in the c-direction indicate that the two-stiffener specimen with 2-inch-wide stiffeners had higher values of compressive strain at corresponding values of applied shear flow than the two-stiffener specimen with 3-inch-wide stiffeners. Surface strain results ϵ_x from back-to-back strain gages oriented parallel to the longitudinal direction of the stiffener are shown in the lower left of the figure. Back-to-back surface strain results in the x-direction indicate that the two-stiffener specimen with 3-inch-wide stiffeners had higher bending strains than the specimen with 2-inch-wide stiffener. The change in slope of the curves for back-to-back surface strain in the x-direction suggests that a redistribution of load occurred in the bead stiffener as the specimens were loaded to failure. Also, the difference in back-to-back surface strain results shown in the figure indicates that significant bending strains occurred as the specimens were loaded to failure.

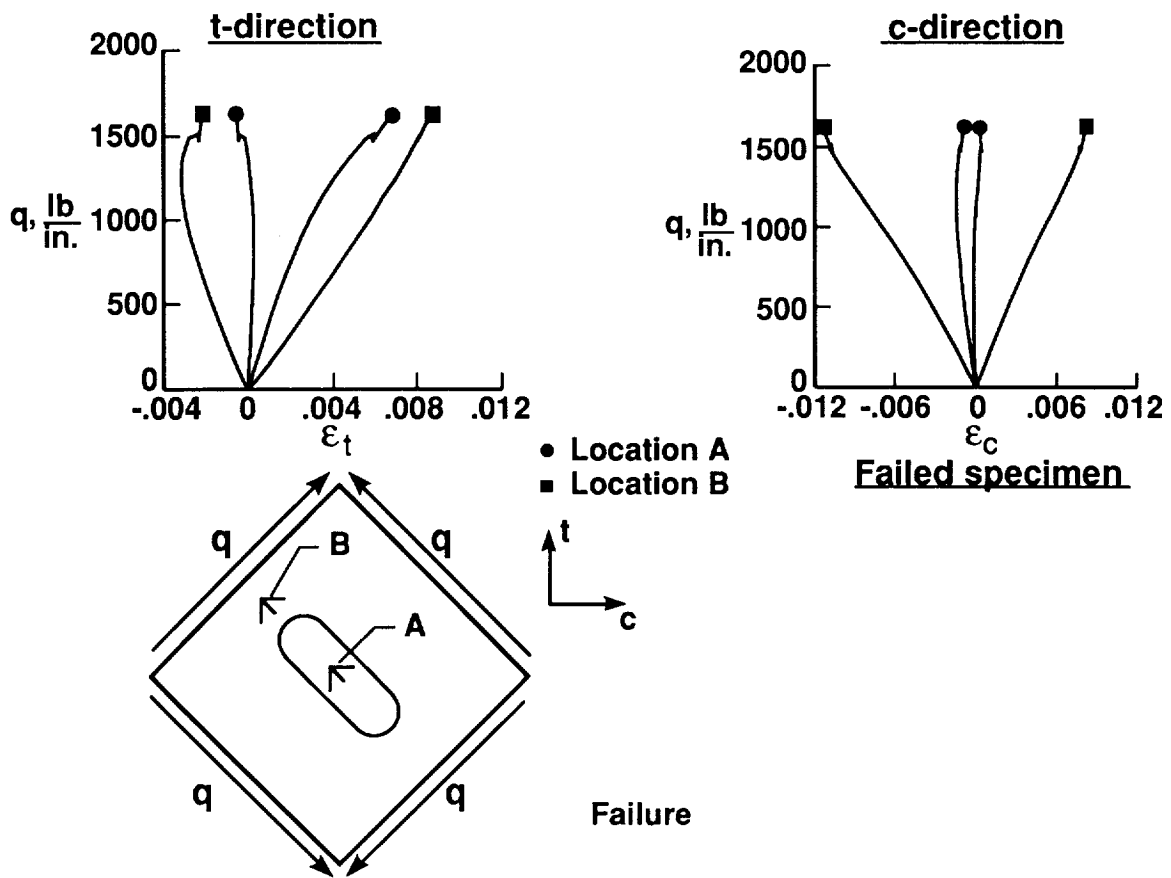


Figure 5

TYPICAL FAILURE CHARACTERISTICS OF BEAD-STIFFENED WEBS

Typical failure characteristics of the bead-stiffened shear webs that were tested are shown in Figure 6. The surface strain results for a one-stiffener specimen are presented in Figure 6 as a function of applied shear flow. The surface strain results were recorded from back-to-back strain gage rosettes at two locations. Surface strain results from strain gage rosettes at Location A, which is near the center of the stiffener, are indicated by the filled circles. Surface strain results from strain gage rosettes at Location B, which is near the end of the stiffener, are indicated by the filled squares. Surface strain measurements ϵ_t from strain gages oriented parallel to the t-direction are shown in the upper left of the figure. Surface strain measurements ϵ_c from strain gages in the c-direction are shown in the upper right of the figure. The surface strain results indicate that much higher tensile and compressive strains occur near the end of the bead stiffener. Also, divergence of the back-to-back strain gage results indicate that higher bending strains occur near the ends of the stiffener than at the center as the specimen was loaded to failure. The bending strains near the end of a stiffener is caused by the eccentricity of the stiffener with respect to the midplane of the test section. A photograph of the failed specimen with one stiffener is shown in the lower right of Figure 6. The failure of the specimen initiated at the end of bead stiffener. The failure was probably caused by the high strains that occur near the end of the stiffener.

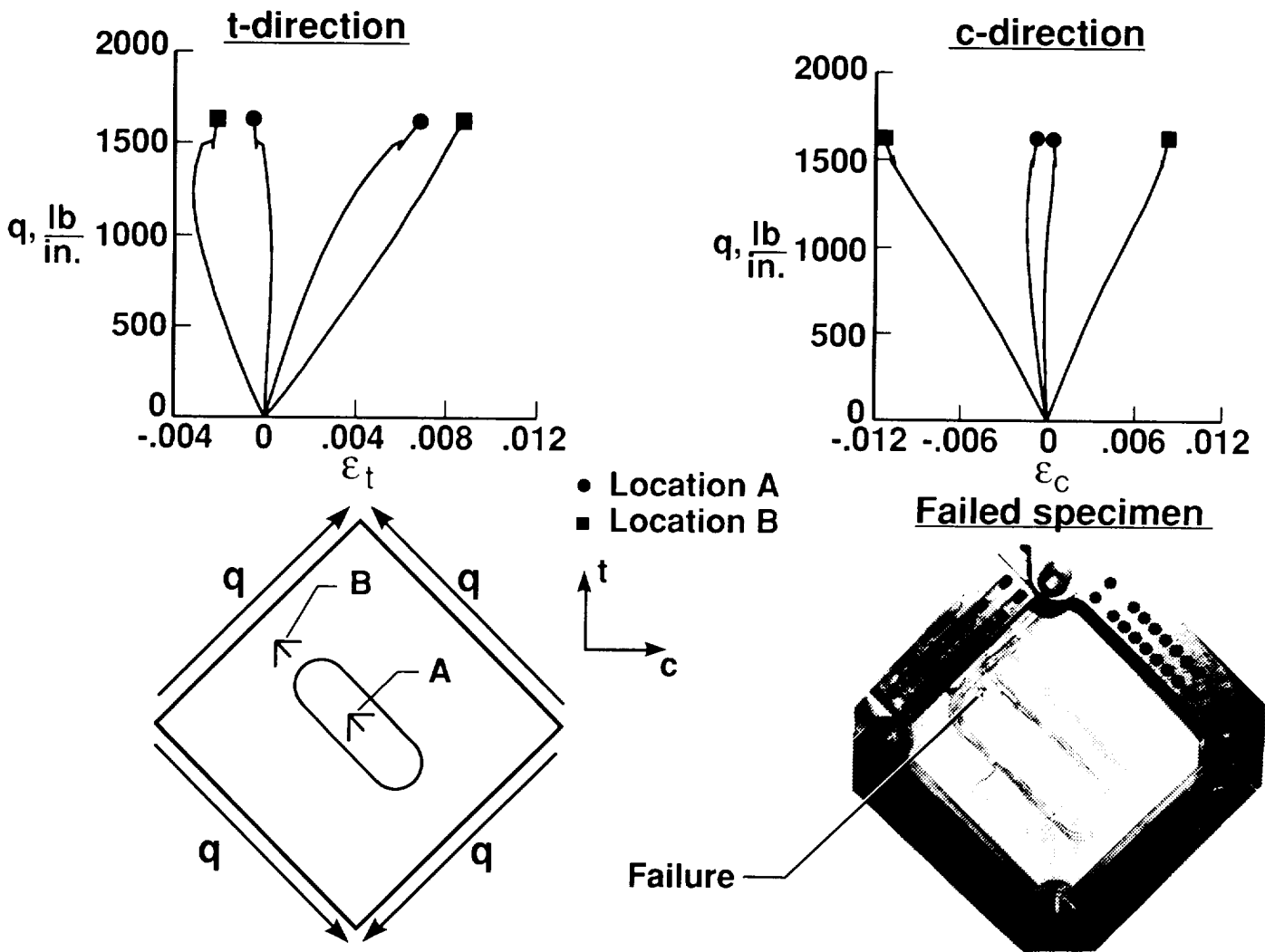


Figure 6

STRESS RESULTANTS DISTRIBUTION IN A BEAD-STIFFENED WEB

Stress resultant contours for a one-stiffener specimen calculated from a geometrically nonlinear finite element analysis at an applied shear flow value of 1553 lb/in. which included transverse shear deformation effects are presented in Figure 7. Contour plots of the inplane normal stress resultants N_x in a direction parallel to the longitudinal direction of the stiffener are shown in the upper left of the figure. The inplane normal stress resultant contour results show that regions of high normal stress resultants exist near the ends of the bead stiffener where failure initiated during the tests. Contour plots of the inplane shear stress resultants N_{xy} are shown in the upper right of the figure. The shear stress resultant contour results show that regions of high shear stress resultants exist near the ends of the bead stiffener and away from the stiffener in the test section area. Contour plots of the transverse shear stress resultants Q_x and Q_y are shown in the lower left and right of the figure, respectively. The transverse shear stress resultant Q_x contours show regions of high transverse shear stress resultants occur near the ends of the bead stiffener. The transverse shear stress resultant Q_y contours show regions of high transverse shear stress resultants occur near to and along the edges where the bead stiffener intersects with the skin. The stress resultant contour results suggest that the stiffener eccentricity causes significant local transverse shear stress resultants in a bead-stiffened shear web.

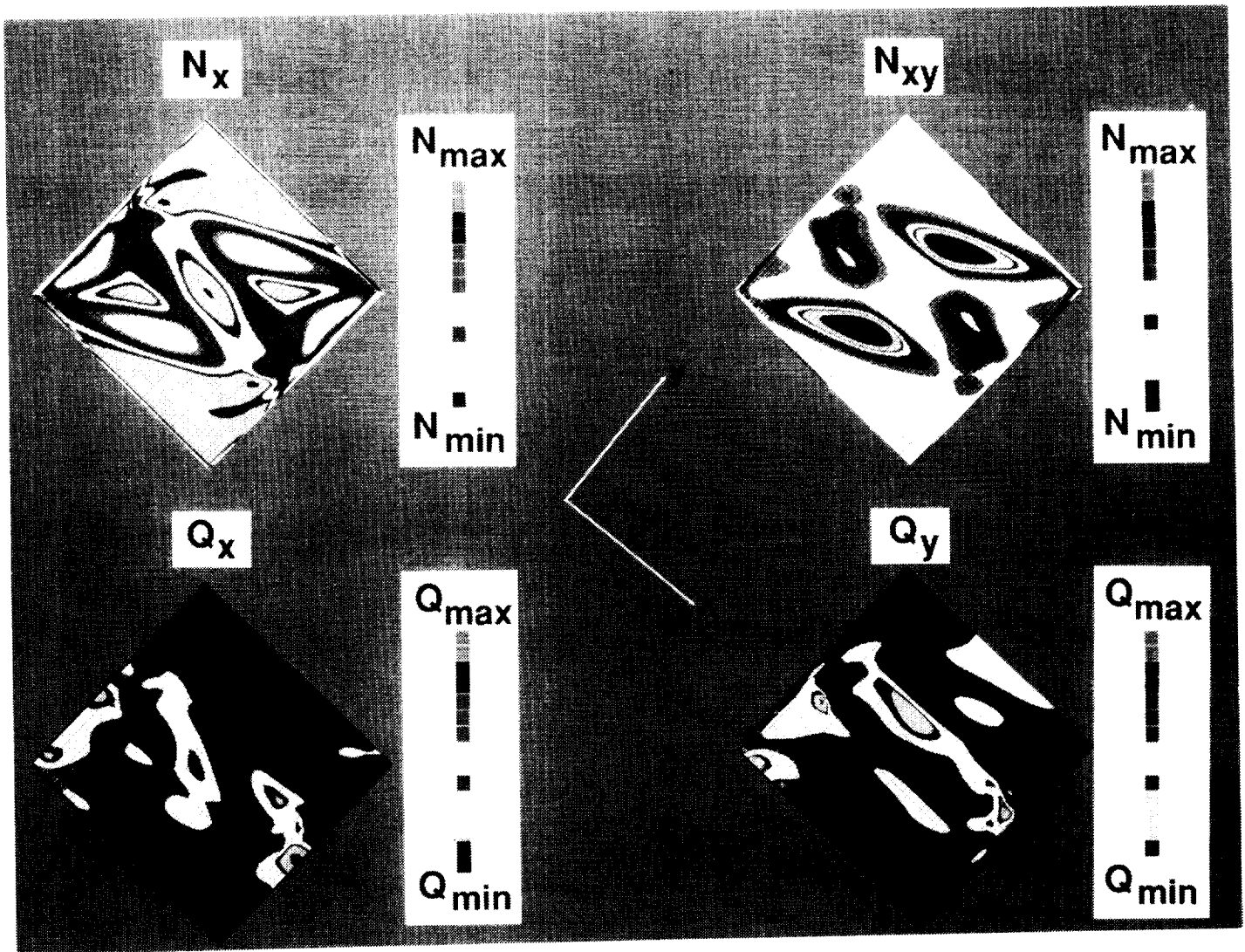


Figure 7

CONCLUDING REMARKS

An experimental and analytical investigation has been conducted to study the structural response and failure characteristics of bead-stiffened graphite-thermoplastic shear webs. Results are presented for specimens with one and two stiffeners. Results are presented for specimens with different bead stiffener widths. Results from a nonlinear finite element analysis are also presented that describe inplane and transverse stress resultant distribution of a bead-stiffened composite plate loaded in shear. Experimental results suggest that bead-stiffened shear webs have a nonlinear response when loaded to failure. Surface strain results suggest that bending strains occur near the bead stiffener when loaded to failure. Analytical results suggest that stiffener eccentricity causes significant local transverse shear stress resultants to occur in bead-stiffened webs. The bead-stiffened webs failed near the end of the stiffener where analysis indicates that significant inplane stress resultants exist.

REFERENCES

1. Jegley, Dawn C.: Compression Behavior of Graphite-Thermoplastic Panels with Circular Holes or Impact Damage. 8th DOD/NASA/FAA Conference on Fibrous Composites in Structural Design, November 28-30, 1989. NASA CP-3087, September 1990.
2. Rouse, Marshall: Effect of Cutouts or Low-speed Impact Damage on the Postbuckling Behavior of Composite Plates Loaded in Shear. AIAA Paper NO. 90-0966; Proceedings of AIAA/ASME/ASCE/ASH/ASC 31st Structures, Structural Dynamics and Materials Conference, Long Beach, CA, April 1990.
3. Stewart, C. B.: The Computational Structural Mechanics Testbed User's Manual. NASA TM-100644, October 1989.

